

## Composition-dependent interatomic potentials: A systematic approach to modelling multicomponent alloys

B. Sadigh<sup>a</sup>, P. Erhart<sup>a</sup>, A. Stukowski<sup>b</sup>, and A. Caro<sup>a</sup>

<sup>a</sup> *Condensed Matter and Materials Division, Lawrence Livermore National Laboratory, Livermore, CA;* <sup>b</sup> *Institut für Materialwissenschaft, Technische Universität Darmstadt, Germany*

(Received 15 July 2009; final version received 27 August 2009)

We propose a simple scheme to construct composition-dependent interatomic potentials for multicomponent systems that when superposed onto the potentials for the pure elements can reproduce not only the heat of mixing of the solid solution in the entire concentration range but also the energetics of a wider range of configurations including intermetallic phases. We show that an expansion in cluster interactions provides a way to systematically increase the accuracy of the model, and that it is straightforward to generalise this procedure to multicomponent systems. Concentration-dependent interatomic potentials can be built upon almost any type of potential for the pure elements including embedded atom method (EAM), modified EAM, bond-order, and Stillinger-Weber type potentials. In general, composition-dependent  $N$ -body terms in the total energy lead to explicit  $N + 1$ -body forces, which potentially renders them computationally expensive. We present an algorithm that overcomes this problem and that can speed up the calculation of the forces for composition-dependent pair potentials in such a way as to make them computationally comparable in efficiency and scaling behaviour to standard EAM potentials. We also discuss the implementation in Monte-Carlo simulations. Finally, we exemplarily review the composition-dependent EAM model for the Fe–Cr system [PRL **95**,075702, (2005)].

**Keywords:** empirical potentials; multicomponent alloys; concentrated alloys; computer simulations; molecular dynamics; Monte Carlo; composition dependent interatomic potentials; cluster interactions

### 1. Introduction

Twenty-five years ago, the Finnis-Sinclair many body potential [1], the Embedded Atom Model of Daw and Baskes [2], the Glue model of Ercolessi and Parrinello [3], and the effective medium theory due to Puska, Nieminen and Norskov [4, 5] marked the birthday of modern atomic scale computational materials science, enabling computer simulations at the multimillion atom scale to become a routine in modern materials science research. This family of many body potentials share in common the fact that the expression for the total energy has non linear contributions of pair functions, removing in this way the limitations of the pair potential formulation to describe realistic elastic properties.

Alloys and compounds, where the thermodynamic information is of relevance, is one of the main fields in which these potentials have been applied. In the early days of many body potentials the main alloy property fitted was the heat of solution of a single impurity [6], *i.e.* the dilute limit of the heat of formation (HOF) of the alloy. However, when these potentials are applied to concentrated alloys the predictions are usually uncontrolled; they work well for systems with a mixing enthalpy that is nearly symmetric and positive over the entire concentration range, as for example in the cases of Fe–Cu [7, 8], or Au–Ni [6, 9, 10].

Alloys which show a strong asymmetry or even a sign inversion in the HOF such

as Fe–Cr or Pd–Ni are beyond the scope of standard many body potential models, and there is not yet a unique methodology suitable for their description. Similar limitations apply with respect to systems with a negative HOF which feature intermetallic phases. Frequently, such systems require different parametrisations for different phases, as in the case of Ni–Al with the B2 phase on one hand [11], and the  $\gamma$  and  $\gamma'$  phases on the other [12].

Two schemes have been developed to deal with these shortcomings in the case of Fe–Cr which displays an inversion in the HOF as a function of concentration, namely the composition-dependent embedded atom method (CD-EAM) [13] and the two-band model (2BM) [14]. For neither one of these schemes, it is obvious how it can be extended to more than two components.

The objective of this paper is to develop a framework for constructing interatomic potential models for multicomponent alloys based on an expansion in clusters of increasing size that can be practically implemented and systematically improved. Our methodology allows to describe systems with arbitrary heat of mixing curves and includes intermetallic phases in a systematic and physically meaningful fashion. Thereby, we overcome the most important disadvantages of current alloy potential schemes and provide a framework for systems of arbitrary complexity.

In our methodology the interatomic interactions are modified by composition-dependent functions. This introduces a dependence on the environment which is somewhat reminiscent of the bond-order potential (BOP) scheme developed by Abell and Tersoff [15–17]. In this formalism the attractive pair potential is scaled by a (usually) angular dependent function (the “bond-order”) which describes the local structure. Thereby, it is possible to distinguish different lattice structures (face-centred cubic, body-centred cubic, cubic diamond *etc.*) and also to stabilise structures with low packing density such as diamond or zincblende lattices. (In fact, the BOP formalism has been successfully applied to model alloys such as Fe–Pt that feature intermetallic phases with different lattice structures [18]). The composition-dependent interatomic potential (CDIP) scheme introduced in the present work and the BOP formalism thus both include explicit environment-dependent terms. However, in the CDIP approach this environment-dependence is used to distinguish different *chemical* motifs while in the BOP scheme it is used to identify different *structural* motifs.

This paper is organised as follows: In Sect. 2.1 we introduce the basic terminology and present a systematic approach to fitting potentials for binary systems. Section 2.2 describes how by including higher order terms it is possible to fit e.g., intermetallic phases. In Sect. 3.1 a series expansion is developed which generalises the concepts introduced in the previous sections and which is used in Sect. 3.2 to obtain explicit expressions for a ternary system. The efficient computation of forces is discussed in Sect. 4 and an optimal implementation in Monte-Carlo simulations is the subject of Sect. 5. Finally, as an example, the composition-dependent embedded atom method potential for Fe–Cr is reviewed in Sect. 6.

## 2. Binary Systems

### 2.1. Pair Potentials

For the sake of clarity of the following exposition, we assume EAM models throughout this paper. It is important to stress that the formalism to be developed hereafter can be applied to any potential model for the pure elements including modified embedded atom method (MEAM) [19, 20], bond-order [15–17], and Stillinger-Weber type [21] potentials.

Consider a single-component system of atoms  $A$ , whose interactions are described by the EAM model,

$$E_A = \sum_i U_A(\bar{\rho}_i) + \frac{1}{2} \sum_i \sum_j \phi_A(r_{ij}) \quad \text{with} \quad \bar{\rho}_i = \sum_{j \neq i} \rho(r_{ij}). \quad (1)$$

The first term in Eq. (1) contains the embedding function  $U_A(\bar{\rho}_i)$ , which is a nonlinear function of the local electron density  $\bar{\rho}_i$  around atom  $i$ . It accounts for cohesion due to band formation in the solid state and is constructed to reproduce the equation of state of system  $A$ . The second term represents the remainder of the interaction energy. It can be interpreted as the effective screened Coulomb interaction between pairs of ions in  $A$ . The EAM formalism can capture the energetics associated with density fluctuations in the lattice and has been successfully applied for modelling the formation of crystal defects such as vacancies, interstitials and their clusters.

Consider now a binary system, where the pure phases are described by EAM potentials. It can be shown that the total energy expression for this type of potentials is invariant under certain scaling operations [22]. This “effective pair format” can be used to rescale the two EAM potentials, e.g. such that at the equilibrium volume for a certain lattice the electron density is 1, to ensure their compatibility. One part of the total energy of the two-component system can be written as the superposition of the respective embedding terms and effective pair interactions:

$$\begin{aligned} E_0 = & \sum_{i \in A} U_A(\bar{\rho}_i^A + \mu_{A(B)} \bar{\rho}_i^B) + \frac{1}{2} \sum_{i \in A} \sum_{j \in A} \phi_A(r_{ij}) \\ & + \sum_{i \in B} U_B(\bar{\rho}_i^B + \mu_{B(A)} \bar{\rho}_i^A) + \frac{1}{2} \sum_{i \in B} \sum_{j \in B} \phi_B(r_{ij}), \end{aligned} \quad (2)$$

where

$$\bar{\rho}_i^S = \sum_{j \in S, j \neq i} \rho^S(r_{ij}). \quad (3)$$

Note that above we have not yet added any explicit  $A-B$  interactions. Equation (2) is a strict superposition of the interatomic potentials for the pure elements with the only caveat that the electron density of the  $A$  ( $B$ ) species in the embedding function of a  $B$  ( $A$ ) particle is scaled with a parameter  $\mu_{B(A)}$  in order to account for the different local electron densities. Thereby, two EAM models can be calibrated with respect to each other. More elaborate schemes are possible, e.g. one can treat  $\mu_A$  and  $\mu_B$  as free parameters. Here for the sake of simplicity, we restrict ourselves to normalised electron densities.

Starting from a parametrisation for  $E_0$ , we now devise a practical scheme for systematically improving the interaction model. Let us denote the true many-body energy functional of the binary system by  $E_t$ . Our goal is to construct an interatomic potential model for the difference energy functional  $\Delta E^{(0)} = E_t - E_0$ . We begin with the two dilute limits. Consider a lattice of  $A$  particles and substitute the atom residing in the  $i$ -th site with a  $B$  atom. Let us now assume that  $\Delta E^{(0)}$  for this configuration can be satisfactorily represented by a pair potential between

the  $A - B$  pairs. In this limit  $\Delta E^{(0)}$  can thus be written as

$$\Delta E^{(0)}(A\text{-rich}) = \sum_{j \in A} V_{AB}^A(r_{ij}). \tag{4}$$

(There is only one sum in this expression since we are dealing with a configuration that contains only one  $B$  atom). A similar expression is obtained for the  $B$ -rich limit

$$\Delta E^{(0)}(B\text{-rich}) = \sum_{j \in B} V_{AB}^B(r_{ij}). \tag{5}$$

Since we do not require the pair potential models for the two dilute limits to coincide with each other, an interpolation is needed which preserves the energetics of the impurities. The main objective of the present paper is to devise such an interpolation scheme. The simplest ansatz for such an expression is

$$\Delta E^{(0)} = \sum_{i \in A} \sum_{j \in B} x_{ij}^A V_{AB}^A(r_{ij}) + \sum_{i \in A} \sum_{j \in B} x_{ij}^B V_{AB}^B(r_{ij}) \tag{6}$$

Above,  $x_{ij}^S$  denotes the concentration of species  $S$  in the neighbourhood of an  $A - B$  pair residing on the  $i$  and  $j$  sites. Ideally, we require this quantity to be easy to calculate and to be insensitive to the local density and topology, in other words it should separate chemistry from structure. In any case,  $x_{ij}^S$  has to represent an average over the neighbourhood of both centres  $i$  and  $j$ . Before we derive the expression for  $x_{ij}^S$ , it is instructive to discuss the corresponding one-centre quantity  $x_i^S$ . It describes the local concentration of species  $S$  around atom  $i$ . A simple way to determine  $x_i^S$  is to choose a local density function  $\sigma(r_{ij})$  and then to evaluate the following expression

$$x_i^S = \frac{\sum_{(j \in S, j \neq i)} \sigma(r_{ij})}{\sum_{j \neq i} \sigma(r_{ij})} = \frac{\bar{\sigma}_i^S}{\bar{\sigma}_i}, \tag{7}$$

which is indeed rather insensitive to the local geometry. This is most obvious in the dilute limits. The local concentration  $x_i^S$  at the site of an impurity atom  $i$  is either 0 (if  $S$  is the minority species) or 1 (if  $S$  is the majority species) independent of the local structure. This is, however, strictly true only for the impurity atom. For the other atoms in the system  $x_j^S$  varies between 0 and 1 depending on the distance to the impurity atom. Also for these particles, atomic displacements may change the value of  $x_j^S$ . A total decoupling of chemistry and structure is therefore not possible. The optimal choice for  $\sigma(r_{ij})$  is the function that minimises the effect of local geometry on  $x_i^S$ . Although it is possible to choose different  $\sigma$ -functions for the different species, we do not expect the quality of the final potential to depend crucially on the choice of  $\sigma(r_{ij})$ . In fact, we expect the best choice for  $\sigma(r_{ij})$  to be the simplest one.

It is now straightforward to extend Eq. (7) to define the concentration  $x_{ij}^S$  in the neighbourhood of a pair of atoms residing on sites  $i$  and  $j$ . To this end, we first define a quantity  $x_{i(j)}^S$  to represent the concentration of the species  $S$  in the

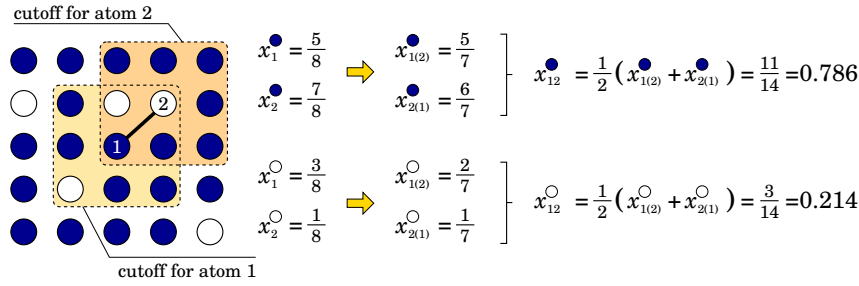


Figure 1. Schematic illustration of the connection between  $x_i^S$  and two-centre concentrations  $x_{ij}^S$  and their computation in a binary alloy according to Eqs. (7) and (8). Here, the cutoff function  $\sigma(r)$  which appears in Eq. (7) is assumed to be a step function which is 1 for  $r < r_c$  and zero otherwise.

neighbourhood of atom  $i$  excluding atom  $j$ :

$$\begin{aligned}
 x_{i(j)}^S &= \frac{\sum_{(k \in S, k \neq i, k \neq j)} \sigma(r_{ik})}{\sum_{(k \neq i, k \neq j)} \sigma(r_{ik})} = \frac{\bar{\sigma}_i^S - \delta(S, t_j) \sigma(r_{ij})}{\bar{\sigma}_i^S - \sigma(r_{ij})} \quad (8) \\
 &= x_i^S \begin{cases} \frac{1 - \sigma(r_{ij})/\bar{\sigma}_i^S}{1 - \sigma(r_{ij})/\bar{\sigma}_i^S} & t_j = S \\ 1 & t_j = O \end{cases},
 \end{aligned}$$

where  $t_i$  denotes the type of atom  $i$ , and  $\delta(t_i, t_j)$  is 1 if  $t_i = t_j$  and zero otherwise. Using this quantity, the two-centre concentration  $x_{ij}^S$  can be defined as follows

$$x_{ij}^S = \frac{1}{2} (x_{i(j)}^S + x_{j(i)}^S) \quad (9)$$

Hence, the two-centre concentration of the species  $S$  about the atom pair  $(i, j)$  is the average concentration in the two separate neighbourhoods of sites  $i$  and  $j$  excluding both of these atoms. This definition, which is illustrated in Fig. 1, has the important advantage that the interpolation scheme introduced in Eq. (6) does not modify the interactions in the dilute limits, since  $x_{ij}^S$  is strictly 0 or 1 in the two limits irrespective of the local structure. Furthermore, it is straightforward to generalise Eq. (9) to multi-centre concentrations. For example, in the next section, we will explicitly discuss the construction of interatomic potentials using three-centre concentrations.

Let us now revisit Eq. (6). As mentioned earlier this is the simplest ansatz for  $\Delta E^{(0)}$  that can reproduce the energetics of both dilute limits. A more general expression is

$$\Delta E^{(0)} = \sum_{i \in A} \sum_{j \in B} h_{AB}^A(x_{ij}^A) V_{AB}^A(r_{ij}) + \sum_{i \in A} \sum_{j \in B} h_{AB}^B(x_{ij}^B) V_{AB}^B(r_{ij}), \quad (10)$$

where  $h_A^B(x)$  and  $h_B^A$  are nonlinear functions with the property  $h_A^B(0) = h_B^A(0) = 0$  and  $h_A^B(1) = h_B^A(1) = 1$ . By fitting these functions to the energetics of the concentrated alloys, the quality of the interatomic potential model for the binary can be improved drastically.

In principle, one can stop here and have an interatomic potential model,  $E_0 + \Delta E^{(0)}$ , that can reproduce the energetics of the dilute limits as well as the solid solution of the binary. It is, however, also possible to further refine the above model.

For this purpose, let us again define a difference energy functional

$$\Delta E^{(1)} = E_t - E_0 - \Delta E^{(0)}, \quad (11)$$

and construct an interatomic potential model for the energy functional  $\Delta E^{(1)}$ . Consider a lattice of  $A$  particles and substitute two atoms, say  $i$  and  $j$ , with  $B$  particles. Assume that  $\Delta E^{(1)}$  for this configuration can be well represented by a potential model describing the interaction of the  $B$ - $B$  pair with a lattice of  $A$  particles. In this limit we can express  $\Delta E^{(1)}$  as

$$\Delta E^{(1)}(A\text{-rich}) = V_{BB}^A(r_{ij}) + \sum_k V_{BBA}^A(r_{ijk}), \quad (12)$$

where  $r_{ijk}$  is shorthand for the three sets of positions of the  $i$ ,  $j$  and  $k$  atoms, i.e.  $\{\mathbf{r}_i, \mathbf{r}_j, \mathbf{r}_k\}$ . In the same way we obtain for the  $B$ -rich limit

$$\Delta E^{(1)}(B\text{-rich}) = V_{AA}^B(r_{ij}) + \sum_k V_{AAB}^B(r_{ijk}). \quad (13)$$

Note that  $\Delta E^{(1)}$  has both a two-body and a three-body component and thus can be decomposed as follows

$$\Delta E^{(1)} = \Delta E_{\text{pair}}^{(1)} + \Delta E_{\text{triplet}}^{(1)}. \quad (14)$$

In the next section we discuss how to incorporate the three-body contribution into the interatomic potential model. For now, we only consider  $\Delta E_{\text{pair}}^{(1)}$ . Following the same line of arguments that lead to Eq. (10), we obtain the expression

$$\Delta E_{\text{pair}}^{(1)} = \sum_{i \in B} \sum_{j \in B} h_{BB}^A(x_{ij}^A) V_{BB}^A(r_{ij}) + \sum_{i \in A} \sum_{j \in A} h_{AA}^B(x_{ij}^B) V_{AA}^B(r_{ij}), \quad (15)$$

which reproduces the contributions of the pair terms in the two limits given by Eqs. (12) and (13). The two non-linear functions have to fulfil the conditions

$$h_{AA}^B(0) = h_{BB}^A(0) = 0 \quad (16)$$

$$h_{AA}^B(1) = h_{BB}^A(1) = 1. \quad (17)$$

By fitting the functions  $h_{AA}^B$  and  $h_{BB}^A$  in the intermediate concentration range to the energetics of the concentrated alloy, one can obtain a further improvement for the interaction model for the binary system.

## 2.2. Beyond Pair Potentials

In this section, we show that the formalism introduced in the previous section can be extended to multi-body interaction potentials, which enables us to capture the energetics of a wider range of phases including ordered compounds. In the previous section, we outlined a scheme to construct composition-dependent pair potentials for the potential energy landscape  $E_0 + \Delta E^{(0)} + \Delta E^{(1)}$ . It was also observed that a proper formulation of  $\Delta E^{(1)}$  requires incorporation of explicit three-body terms. In this section we describe how to construct such composition-dependent multi-body potentials.

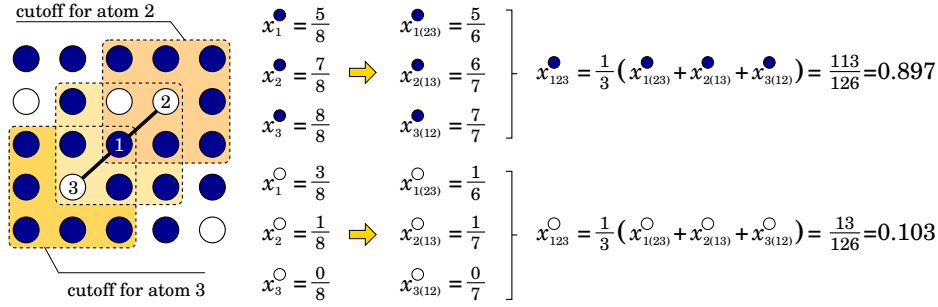


Figure 2. Schematic illustration of the computation of three-centre concentrations in a binary alloy using Eqs. (7) and (21). Here, the cutoff function  $\sigma(r)$  which appears in Eq. (7) is assumed to be a step function which is 1 for  $r < r_c$  and zero otherwise.

First, we require an interpolation scheme to connect the two limits of the three-body term  $\Delta E_{\text{triplet}}^{(1)}$  in Eq. (14). The simplest ansatz for such an expression is

$$\Delta E_{\text{triplet}}^{(1)} = \sum_{i \in B} \sum_{j \in B} \sum_{k \in A} x_{ijk}^A V_{BBA}^A(r_{ijk}) + \sum_{i \in A} \sum_{j \in A} \sum_{k \in B} x_{ijk}^B V_{AAB}^B(r_{ijk}), \quad (18)$$

where  $x_{ijk}^S$  denotes the concentration of species  $S$  in the neighbourhood of the triplet residing on sites  $i, j$  and  $k$ . In analogy with the derivation of the two-centre concentration Eq. (9), we start from the one-centre concentration  $x_i^S$  and define the intermediate quantity  $x_i^S(jk)$  that represents the concentration centred around atom  $i$  excluding atoms  $j$  and  $k$

$$x_{i(jk)}^S = \frac{\sum_{(l \in S, l \neq i, l \neq j, l \neq k)} \sigma(r_{il})}{\sum_{(l \neq i, l \neq j, l \neq k)} \sigma(r_{il})} = \frac{\bar{\sigma}_i^S - \delta(S, t_j)\sigma(r_{ij}) - \delta(S, t_k)\sigma(r_{ik})}{\bar{\sigma}_i^S - \sigma(r_{ij}) - \sigma(r_{ik})} \quad (19)$$

$$= x_i^S \frac{1 - [\delta(S, t_j)\sigma(r_{ij}) + \delta(S, t_k)\sigma(r_{ik})] / \bar{\sigma}_i^S}{1 - [\sigma(r_{ij}) + \sigma(r_{ik})] / \bar{\sigma}_i^S}, \quad (20)$$

and now following the same line of arguments leading to Eq. (9) we define the three-centre concentration  $x_{ijk}^S$  as follows

$$x_{ijk}^S = \frac{1}{3} \left( x_{i(jk)}^S + x_{j(ik)}^S + x_{k(ij)}^S \right). \quad (21)$$

A graphical illustration of the computation of this quantity is given in Fig. 2. The three-centre concentration of the species  $S$  about the triplet  $(i, j, k)$  is the average concentration (excluding the triplet) in three separate neighbourhoods, each of which is centred at one of the atoms in the triplet. Thanks to this definition  $x_{ijk}^S$  is strictly 0 or 1 in the two dilute limits described in Eqs. (12) and (13), irrespective of the local structure. Hence, the interpolation scheme in Eq. (18) does not alter the interactions in Eqs. (12) and (13). Again, as in Eq. (10), we can improve the simple interpolation scheme in Eq. (18)

$$\Delta E_{\text{triplet}}^{(1)} = \sum_{i \in B} \sum_{j \in B} \sum_{k \in A} h_{BBA}^A(x_{ijk}^A) V_{BBA}^A(r_{ijk}) + \sum_{i \in A} \sum_{j \in A} \sum_{k \in B} h_{AAB}^B(x_{ijk}^B) V_{AAB}^B(r_{ijk}), \quad (22)$$

where  $h_{BBA}^A$  and  $h_{AAB}^B$  are non-linear functions that can be fitted to the energetics of the concentrated alloys with the boundary conditions

$$h_{BBA}^A(0) = h_{AAB}^B(0) = 0 \quad \text{and} \quad h_{BBA}^A(1) = h_{AAB}^B(1) = 1. \quad (23)$$

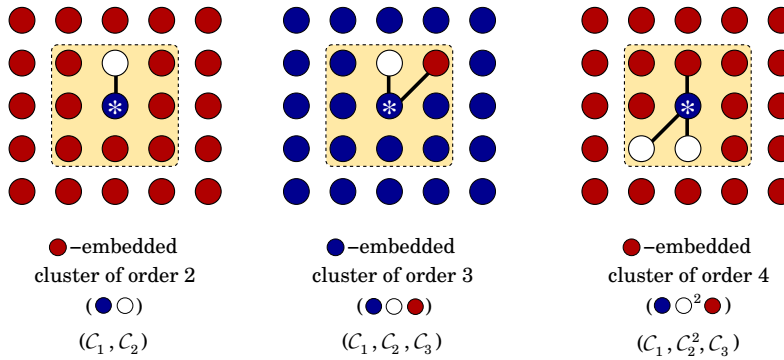


Figure 3. Schematic illustration of  $\mathcal{S}$ -embedded coloured clusters of orders 2, 3, and 4 in a ternary alloy. The shaded region indicates the cutoff range around the central atom marked by an asterisk.

Following this scheme composition-dependent cluster interactions of arbitrary order can be included in the interatomic potential model. To summarise, to incorporate cluster interactions of order  $n$ , two cluster potentials are constructed, one for the configuration where the cluster is embedded in the  $A$  lattice and one for the configuration where the cluster is embedded in the  $B$  lattice. Subsequently these limits are interpolated using the  $n$ -centre concentrations. In the next section, we review this strategy in detail to show that a systematic series expansion in composition-dependent cluster interactions is possible for general multicomponent systems.

### 3. Multicomponent Systems

#### 3.1. Series Expansion in Embedded Cluster Interactions

In the first sections of this paper, we have shown how to practically construct interatomic potentials for binary systems. First, mixed interatomic pair and triplet potentials are generated for the dilute limits which are subsequently extended to arbitrary concentrations by fitting interpolation functions that depend on the local concentration about the atomic pairs and triplets. The choice of specific potentials and dilute configurations was mainly driven by physical intuition. In this section we show that this procedure can be formalised and generalised to arbitrarily complex systems with more than two components.

Consider an  $n$ -component mixture of  $N$  particles that are distinguishable only through their species. Assign a unique colour to each of the species:  $\{\mathcal{C}_1, \dots, \mathcal{C}_n\}$ . We define a colour cluster of order  $m$  to be a set of  $m$  particles with a specific colour combination. We use the occupation number formalism to identify colour schemes, i.e.  $(\mathcal{C}_1^{k_1}, \dots, \mathcal{C}_n^{k_n})$ , where  $k_i$  is the number of particles in the cluster with colour  $\mathcal{C}_i$ , and  $\sum_i k_i = m$ . For example, a cluster of order 3 consisting of one particle with the colour  $\mathcal{C}_1$  and two particles with the colour  $\mathcal{C}_3$ , is denoted by  $(\mathcal{C}_1, \mathcal{C}_3^2)$ . Furthermore, we define an  $\mathcal{S}$ -embedded colour cluster of order  $m$  to be a set of  $m$  coloured particles embedded in a pure matrix of species  $\mathcal{S}$ . Three examples of such  $\mathcal{S}$ -embedded coloured clusters are shown in Fig. 3. The key idea is that the potential energy landscape of an alloy can be expanded in the basis set of elementary interaction potentials each of which is constructed to reproduce the energetics of a particular embedded colour cluster. The order of an interaction element in the series is determined by the order of the corresponding colour cluster. By progressively including higher order colour cluster interactions, one can systematically increase the accuracy of the model.

To recapitulate, we expand the potential energy landscape of multicomponent systems in the basis set of colour cluster interatomic potential functions



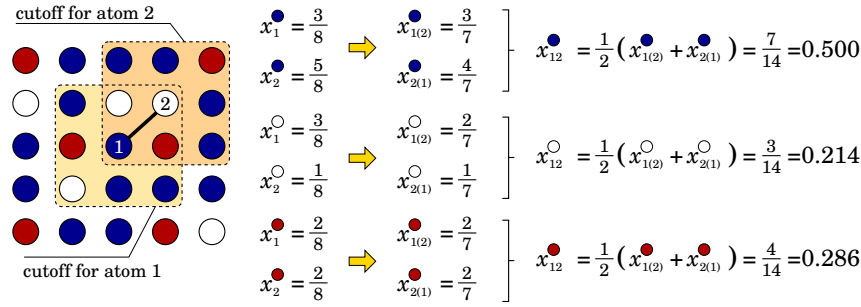


Figure 4. Schematic illustration of the connection between  $x_i^S$  and two-centre concentrations  $x_{ij}^S$  and their computation in a ternary alloy according to Eqs. (7) and (8). Here, the cutoff function  $\sigma(r)$  which appears in Eq. (7) is assumed to be a step function which is 1 for  $r < r_c$  and zero otherwise.

$V_{C_1^{k_1} \dots C_n^{k_n}}^S(\{\mathbf{r}\})$ , where  $\{\mathbf{r}\}$  is the real-space configuration of the respective cluster. The expansion coefficient for each basis function is the interpolation function  $h_{C_1^{k_1} \dots C_n^{k_n}}^S(x^S)$ , where  $x^S$  is the local concentration of the species  $S$  in the neighbourhood of the cluster. One of the innovations in this work is a simple and computationally expeditious way to determine  $x^S$  which is illustrated for the case of a ternary alloy in Fig. 4. Formally the total energy expression for an alloy of  $n$  components and  $N$  particles can be written as

$$E = E_0 + \sum_m \underbrace{\sum_{k_1} \dots \sum_{k_n}}_{\sum_{i=1}^n k_i = m} \sum_S h_{C_1^{k_1} \dots C_n^{k_n}}^S(x^S) V_{C_1^{k_1} \dots C_n^{k_n}}^S(\{\mathbf{r}\}), \quad (24)$$

where the first sum is over the order of the cluster potentials and the subsequent sums are over all distinguishable colour combinations of  $m$ -size clusters. Each term in the above expansion can be evaluated as follows

$$h_{C_1^{k_1} \dots C_n^{k_n}}^S(x^S) V_{C_1^{k_1} \dots C_n^{k_n}}^S(\{\mathbf{r}\}) = \underbrace{\sum_{i_1=1}^N \dots \sum_{i_m=1}^N}_{\{i_1 \dots i_m\} \in \{C_1^{k_1} \dots C_n^{k_n}\}} h_{C_1^{k_1} \dots C_n^{k_n}}^S(x_{i_1 \dots i_m}^S) V_{C_1^{k_1} \dots C_n^{k_n}}^S(r_{i_1 \dots i_m}). \quad (25)$$

The sums in Eq. (25) are over all possible  $m$ -size atom clusters  $\{i_1 \dots i_m\}$  in the system with the colour scheme  $(C_1^{k_1}, \dots, C_n^{k_n})$ .

The main advantage of this scheme is that the basis functions can be constructed sequentially and independent of the interpolation functions. The lower order terms can be constructed with no knowledge of the higher order terms and therefore need not be reparametrised when higher order cluster potentials are constructed. The higher order terms in the expansion become progressively smaller. Furthermore, addition of new terms in the series expansion is not likely to introduce unphysical behaviour, a problem that plagues most fitting schemes for interatomic potentials.

### 3.2. Explicit expressions for ternary alloys

In this section we illustrate the formal discussion in the previous section by constructing an expansion in embedded pair and triplet potentials for a ternary system. For simplicity we assume the pure elements are described by EAM models. The extension to larger number of components and higher order cluster potentials will be obvious. We consider a system of three components  $A$ ,  $B$  and  $C$ , and assume

that three composition-dependent pair potentials for the binary systems  $A - B$ ,  $A - C$  and  $B - C$  have already been constructed. Explicitly, the  $A - B$  interaction is given by the following expression

$$\begin{aligned}
 E_{A-B}^{pair} = & \sum_{i \in A} U_A (\bar{\rho}_i^A + \mu_{A(B)} \bar{\rho}_i^B) + \frac{1}{2} \sum_{i \in A} \sum_{j \in A} (h_{AA}^A(x_{ij}^A) \phi_A(r_{ij}) + h_{AA}^B(x_{ij}^B) V_{AA}^B(r_{ij})) \\
 & + \sum_{i \in B} U_B (\bar{\rho}_i^B + \mu_{B(A)} \bar{\rho}_i^A) + \frac{1}{2} \sum_{i \in B} \sum_{j \in B} (h_{BB}^B(x_{ij}^B) \phi_B(r_{ij}) + h_{BB}^A(x_{ij}^A) V_{BB}^A(r_{ij})) \\
 & + \sum_{i \in A} \sum_{j \in B} (h_{AB}^A(x_{ij}^A) V_{AB}^A(r_{ij}) + h_{AB}^B(x_{ij}^B) V_{AB}^B(r_{ij})). \tag{26}
 \end{aligned}$$

By now the notation above should be familiar. The interaction potentials for the two other pairs can be written in analogous fashion.

Now, we can spell out the expansion in embedded pair potentials for the ternary  $A - B - C$

$$\begin{aligned}
 E_{A-B-C}^{pair} = & \sum_{i \in A} U_A (\bar{\rho}_i^A + \mu_{A(B)} \bar{\rho}_i^B + \mu_{A(C)} \bar{\rho}_i^C) \tag{27} \\
 & + \sum_{i \in B} U_B (\bar{\rho}_i^B + \mu_{B(A)} \bar{\rho}_i^A + \mu_{B(C)} \bar{\rho}_i^C) \\
 & + \sum_{i \in C} U_C (\bar{\rho}_i^C + \mu_{C(A)} \bar{\rho}_i^A + \mu_{C(B)} \bar{\rho}_i^B) \\
 & + \frac{1}{2} \sum_{i \in A} \sum_{j \in A} [h_{AA}^A(x_{ij}^A) \phi_A(r_{ij}) + h_{AA}^B(x_{ij}^B) V_{AA}^B(r_{ij}) + h_{AA}^C(x_{ij}^C) V_{AA}^C(r_{ij})] \\
 & + \frac{1}{2} \sum_{i \in B} \sum_{j \in B} [h_{BB}^B(x_{ij}^B) \phi_B(r_{ij}) + h_{BB}^A(x_{ij}^A) V_{BB}^A(r_{ij}) + h_{BB}^C(x_{ij}^C) V_{BB}^C(r_{ij})] \\
 & + \frac{1}{2} \sum_{i \in C} \sum_{j \in C} [h_{CC}^C(x_{ij}^C) \phi_C(r_{ij}) + h_{CC}^A(x_{ij}^A) V_{CC}^A(r_{ij}) + h_{CC}^B(x_{ij}^B) V_{CC}^B(r_{ij})] \\
 & + \sum_{i \in A} \sum_{j \in B} [h_{AB}^A(x_{ij}^A) V_{AB}^A(r_{ij}) + h_{AB}^B(x_{ij}^B) V_{AB}^B(r_{ij}) + h_{AB}^C(x_{ij}^C) V_{AB}^C(r_{ij})] \\
 & + \sum_{i \in A} \sum_{j \in C} [h_{AC}^A(x_{ij}^A) V_{AC}^A(r_{ij}) + h_{AC}^B(x_{ij}^B) V_{AC}^B(r_{ij}) + h_{AC}^C(x_{ij}^C) V_{AC}^C(r_{ij})] \\
 & + \sum_{i \in B} \sum_{j \in C} [h_{BC}^A(x_{ij}^A) V_{BC}^A(r_{ij}) + h_{BC}^B(x_{ij}^B) V_{BC}^B(r_{ij}) + h_{BC}^C(x_{ij}^C) V_{BC}^C(r_{ij})].
 \end{aligned}$$

The only unknowns in the above equation are  $V_{AB}^C(r_{ij})$ ,  $V_{AC}^B(r_{ij})$ ,  $V_{BC}^A(r_{ij})$ ,  $h_{AB}^C(x_{ij}^C)$ ,  $h_{AC}^B(x_{ij}^B)$  and  $h_{BC}^A(x_{ij}^A)$ . The potentials  $V_{AB}^C(r_{ij})$ ,  $V_{AC}^B(r_{ij})$  and  $V_{BC}^A(r_{ij})$  describe the interaction between pairs of unlike species embedded in pure lattices of the third species of the ternary. In analogy with the previous section, it is reasonable to expect that we can construct these potentials separately in their respective dilute limits and subsequently fit the interpolation functions  $h_{AB}^C(x_{ij}^C)$ ,  $h_{AC}^B(x_{ij}^B)$ ,  $h_{BC}^A(x_{ij}^A)$  to the energetics of the concentrated ternary alloys. However, when the number of species increases certain complications can arise that are not present in the binaries. This is well illustrated in the situation above. We now show that it is in fact not possible to separately construct the three pair potentials  $V_{AB}^C(r_{ij})$ ,

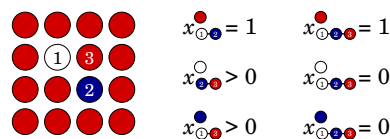


Figure 5. Schematic illustration of two and three-centre concentrations for a ternary alloy in the dilute limit. Note that the two-centre concentrations  $x_{ij}$  in the *dilute limit* in a binary alloy are either one or zero. In contrast, in the case of a ternary alloy the two-centre concentrations in the same limit can be non-zero. The three-centre concentrations, however, are again either one or zero.

$V_{AC}^B(r_{ij})$  and  $V_{BC}^A(r_{ij})$  described above.

To this end, consider a pure lattice of  $N$  particles of e.g.,  $C$  species. Substitute two nearest neighbour particles in this lattice with an  $A$  particle and a  $B$  particle respectively. The ternary energy Eq. (27) for a  $C$ -rich configuration containing one  $A - B$  pair on the sites  $i$  and  $j$  respectively becomes

$$\begin{aligned}
 E_{A-B-C}^{pair}(C\text{-rich}) &= \tilde{E}_0 \\
 &+ \frac{1}{2} \sum_{k \in C} \sum_{l \in C} (h_{CC}^C(x_{kl}^C) \phi_C(r_{kl}) + h_{CC}^A(x_{kl}^A) V_{CC}^A(r_{kl}) + h_{CC}^B(x_{kl}^B) V_{CC}^B(r_{kl})) \\
 &+ V_{AB}^C(r_{ij}) + \sum_{k \in C} (h_{AC}^B(x_{ik}^B) V_{AC}^B(r_{ik}) + h_{AC}^C(x_{ik}^C) V_{AC}^C(r_{ik})) . \\
 &+ \sum_{k \in C} (h_{BC}^A(x_{jk}^A) V_{BC}^A(r_{jk}) + h_{BC}^C(x_{jk}^C) V_{BC}^C(r_{jk})) ,
 \end{aligned}$$

where for the sake of clarity we have replaced the three embedding terms in Eq. (27) by  $\tilde{E}_0$ . Observe that all three unknown potentials  $V_{AC}^C(r_{ij})$ ,  $V_{AC}^B(r_{ik})$  and  $V_{BC}^A(r_{jk})$  as well as their corresponding interpolation functions appear in Eq. (28). This is in contrast to the binary case, e.g. Eqs. (4), (5), (12) and (13), where the potentials for the two dilute limits can be constructed independently of each other. This is because the two-centre concentrations in the *dilute limit* in a *binary* alloy are either one or zero. In contrast, in the case of a *ternary* alloy the two-centre concentrations in the same limit can be non-zero (see Fig. 5).

A straightforward solution to the above problem is to fit all three pair potentials simultaneously. A closer look at Eq. (28), however, suggests a simpler solution. Let us examine the interpolation functions  $h_{AC}^B(x_{ik}^B)$  and  $h_{BC}^A(x_{jk}^A)$ . Note that since we are dealing here with an  $A - B$  cluster in a  $C$ -rich system  $x_{ik}^B$  and  $x_{jk}^A$  are close to zero. Remembering the boundary conditions on the interpolation functions, i.e.  $h(1) = 1$  and  $h(0) = 0$ , we conclude that the contributions of the  $V_{AC}^B(r_{ij})$  and  $V_{BC}^A(r_{ij})$  potentials to the energetics of an  $A - B$  pair embedded in a  $C$  lattice are small. In fact, we can diminish the contribution of these potentials to Eq. (28) by enforcing the interpolation functions to be 0 for  $x < x_{th}$ , where  $x_{th}$  is the largest concentration of  $B$  or  $A$  particles found about any pair in the system. In this way, one can generally separate the construction of cluster potentials when they overlap in the dilute configurations.

The problem of potential overlap in the dilute limit discussed above should not be neglected. On the other hand it is quite benign and —as shown above— can be handled easily. Furthermore, more often than not, even for complex clusters and many components, there is no overlap. We illustrate this point by considering the

simplest expansion in triplet cluster potentials for the ternary above:

$$E_{A-B-C}^{\text{triplet}} = \sum_{i \in A} \sum_{j \in B} \sum_{k \in C} h_{ABC}^A(x_{ijk}^A) V_{ABC}^A(r_{ijk}) \quad (28)$$

$$+ h_{ABC}^B(x_{ijk}^B) V_{ABC}^B(r_{ijk}) + h_{ABC}^C(x_{ijk}^C) V_{ABC}^C(r_{ijk}).$$

Now consider again the same  $C$  lattice as above, where an  $A - B$  pair has been embedded at the sites  $i$  and  $j$ . The triplet energy becomes

$$E_{A-B-C}^{\text{triplet}}(C\text{-rich}) = \sum_{k \in C} V_{ABC}^C(r_{ijk}). \quad (29)$$

Since we have only contributions from  $V_{ABC}^C(r_{ijk})$  for these configurations, we can construct these potentials separately from each other and independent of the interpolation functions. This is because in the dilute limit the three-centre concentrations are again either one or zero (see Fig. 5).

#### 4. Implementation of Forces in Molecular dynamics

Next to accuracy, the most important quality of an interatomic potential model is its computational efficiency when implemented into atomistic simulation codes. Due to the unconventional form of the interatomic potentials described in this work, it is important to discuss the efficient implementation of forces for molecular-dynamics simulations. We will see below that the straightforward derivation of the forces for composition-dependent pair potentials leads to explicit 3-body forces. In fact in general, composition-dependent  $N$ -body potentials lead to explicit  $N + 1$ -body forces. Below we present an algorithm that considerably speeds up the calculation of forces for composition-dependent  $N$ -body potentials, making them comparable in efficiency to the corresponding  $N$ -body regular potentials. In the following, for the sake of clarity we limit our discussion to pair potentials. The extension to cluster potentials of higher order is straightforward.

For reference, let us first consider a conventional mixed pair potential energy expression for a binary system,

$$E_{\text{pp}} = \sum_{i \in A} \sum_{j \in B} V(r_{ij}). \quad (30)$$

Within this model the force on a particle  $k$  of type  $A$  is calculated as follows

$$\frac{\partial E_{\text{pp}}}{\partial \mathbf{r}_k^A} = \sum_{j \in B} V'(r_{kj}) \frac{\mathbf{r}_{kj}}{r_{kj}}. \quad (31)$$

Let us now consider a typical composition-dependent pair potential model for the same binary system,

$$E_{\text{cdpp}} = \sum_{i \in A} \sum_{j \in B} h(x_{ij}^A) V(r_{ij}), \quad (32)$$

where  $x_{ij}^A$  is the two-centre concentration of the species  $A$  about the  $(i, j)$  pair.

Now the force on particle  $k$  of type  $A$  can be written

$$\frac{\partial E_{\text{cdpp}}}{\partial \mathbf{r}_k^A} = \sum_{j \in B} V'(r_{kj}) h(x_{kj}^A) + \sum_{i \in A} \sum_{j \in B} V(r_{ij}) h'(x_{ij}^A) \frac{1}{2} \left( \frac{\partial x_{i(j)}^A}{\partial \mathbf{r}_k^A} + \frac{\partial x_{j(i)}^A}{\partial \mathbf{r}_k^A} \right), \quad (33)$$

for which after some algebra we obtain

$$\frac{\partial x_{i(j)}^A}{\partial \mathbf{r}_k^A} = \frac{\bar{\sigma}_i^B - \delta(\mathcal{S}, t_j) \sigma(r_{ij})}{(\bar{\sigma}_i)^2 - \sigma(r_{ij})} \sigma'(r_{ik}) \frac{\mathbf{r}_{ki}}{r_{ki}}. \quad (34)$$

All the quantities above have already been defined in Eqs. (8) and (9). The second term in Eq. (33) contains contributions from two particles  $i$  and  $j$  to the forces on particle  $k$ . Hence composition-dependent pair potentials lead to explicit three-body forces, which usually implies significantly more expensive to calculations. However, we will now show that in the case of expressions such as Eq. (33) one can regroup the terms in such a way as to speed up the calculation of forces drastically. To this end, let us introduce a per-atom quantity that for an atom of type  $A$  reads

$$M_{i \in A}^{\mathcal{S}} = \sum_{j \in B} V(r_{ij}) h'(x_{ij}^A) \frac{\bar{\sigma}_i^{\mathcal{S}} - \delta(B, t_j) \sigma(r_{ij})}{(\bar{\sigma}_i)^2 - \sigma(r_{ij})}, \quad (35)$$

and for an atom of type  $B$

$$M_{i \in B}^{\mathcal{S}} = \sum_{j \in A} V(r_{ij}) h'(x_{ij}^A) \frac{\bar{\sigma}_i^{\mathcal{S}} - \delta(A, t_j) \sigma(r_{ij})}{(\bar{\sigma}_i)^2 - \sigma(r_{ij})}. \quad (36)$$

Substituting  $M_i^{\mathcal{S}}$  into Eq. (33) we obtain

$$\frac{\partial E_{\text{cdpp}}}{\partial \mathbf{r}_k^A} = \sum_{j \in B} V'(r_{kj}) h(x_{kj}^A) + \frac{1}{2} \sum_i M_i^B \sigma'(r_{ki}) \frac{\mathbf{r}_{ki}}{r_{ki}}. \quad (37)$$

Similar derivation for the force on a particle  $k$  of type  $B$  leads to the expression

$$\frac{\partial E_{\text{cdpp}}}{\partial \mathbf{r}_k^B} = \sum_{j \in A} V'(r_{kj}) h(x_{kj}^A) + \frac{1}{2} \sum_i M_i^A \sigma'(r_{ki}) \frac{\mathbf{r}_{ki}}{r_{ki}}. \quad (38)$$

Each quantity in the above force expressions can be calculated separately via pairwise summations. This allows for a very efficient three-step algorithm for the calculation of forces: (i) compute and store the local partial densities  $\bar{\sigma}_i^{\mathcal{S}}$  for every atom, (ii) compute and store the quantities  $M_i^{\mathcal{S}}$  for every atom, and (iii) compute the forces according to the Eqs. (37) and (38). This method leads to computational efficiency comparable to standard EAM models.

## 5. Linearised Models for efficient Monte-Carlo simulations

Molecular dynamics simulations are limited when it comes to modelling phenomena such as precipitation, surface and grain boundary segregation, or ordering in alloys. Monte-Carlo (MC) methods, however, are ideally suited for such applications. The most common techniques are based on so-called swap trial moves, in which the

chemical identity of a random particle is changed. The resulting change in potential energy,  $\Delta E$ , is used to decide whether the swap is accepted or rejected.

The main task in an MC simulation is therefore to calculate the change in potential energy induced by swapping the type of a single atom. For short-range potentials this can be done very efficiently, since the type exchange only affects the atoms in the neighbourhood of the type swap. In the framework of the standard EAM model the situation is as follows: Changing the species of one atom directly affects (1) its embedding energy, (2) its pair-wise interactions with neighbouring atoms, and (3) indirectly changes the electron density at neighbouring atoms and therefore their embedding energies. All these quantities need to be recalculated by visiting the atoms affected by the type swap.

In the case of composition-dependent models the situation turns out to be more laborious. To illustrate this let us again consider a typical composition-dependent pair potential model for a binary system:

$$E_{\text{cdpp}} = \sum_{i \in A} \sum_{j \in B} h(x_{ij}^A) V(r_{ij}), \quad (39)$$

where  $x_{ij}^A$  is the two-centre concentration of the species  $A$  about the  $(i, j)$  pair

$$x_{ij}^A = \frac{1}{2} \left( x_{i(j)}^A + x_{j(i)}^A \right), \quad (40)$$

where the  $x_{i(j)}^A$  is the local concentration  $A$  about the atom  $i$  excluding atom  $j$ . From Eq. (9) we observed that to a good approximation  $x_{i(j)} \approx x_i$ . Therefore, for the qualitative discussion below we replace  $x_{i(j)}$  by  $x_i$ . In the energy expression Eq. (39), the site energy  $E_i$  of an atom  $i$  does not only depend on the local concentration  $x_i$ , but also on the concentrations  $x_j$  of all its neighbours  $j$ . This has a dreadful impact on the efficiency of the energy calculation. Changing the chemical identity of some atom  $i$  alters the local concentrations  $x_j$  of all its direct neighbours  $j$ , which in turn affects the mixed interaction of all atoms  $j$  with all of their respective neighbour atoms  $k$ . All of these have to be re-evaluated to compute the total change in energy induced by the single swap operation. The interaction radius that has to be considered is therefore twice as large as the cutoff radius of the underlying EAM potential, which increases the computational costs by at least one order of magnitude.

This issue can be resolved quite effectively if we linearise the interpolation function  $h(x_{ij}^A)$  as follows

$$h(x_{ij}^A) = \frac{1}{2} \left( h(x_{i(j)}^A) + h(x_{j(i)}^A) \right). \quad (41)$$

Within the new linearised formulation, although a single pair interaction between two atoms  $j$  and  $k$  still depends on the concentration at both sites, the site energy can be recast in a form that is independent of the concentrations on the neighbouring sites. As a result, the site energy of atom  $k$  is no longer affected by changing the type of an atom  $i$  that is farther away than one cutoff radius. Note that linearisation can be done for interpolation functions of any  $n$ -centre concentrations. All composition-dependent models independent of cluster size can therefore be linearised. We have discussed the linearised model and its implementation for MD and MC at length in a recent publication [23].

## 6. A practical example

To provide a practical illustration of the concepts developed in this paper, we now revisit the composition-dependent EAM potential for Fe–Cr [13], which has already been successfully applied in a number of cases [24, 25].

### 6.1. Application of composition-dependent embedded atom method to Fe–Cr

Iron alloys are materials with numerous technological applications. In particular Fe–Cr alloys are at the basis of ferritic stainless steels. It has been recently shown [26] that the Fe–Cr alloy in the ferromagnetic phase has an anomaly in the heat of formation which shows a change in sign going from negative to positive at about 10% Cr and leads to the coexistence of intermetallic phase [27] and segregation in the same alloy. This complexity results from a “magnetic frustration” of the Cr atoms in the Fe matrix [28] which leads to an effectively repulsive Cr–Cr interaction. Capturing this complexity with an empirical potential model has been an active subject of research in recent years.

To model this system, Caro and coworkers used the following ansatz

$$\begin{aligned}
 E_{\text{Fe-Cr}} = & \sum_{i \in \text{Fe}} U_{\text{Fe}} (\bar{\rho}_i^{\text{Fe}} + \bar{\rho}_i^{\text{Cr}}) + \frac{1}{2} \sum_{i \in \text{Fe}} \sum_{j \in \text{Fe}} \phi_{\text{Fe}}(r_{ij}) \\
 & + \sum_{i \in \text{Cr}} U_{\text{Cr}} (\bar{\rho}_i^{\text{Cr}} + \bar{\rho}_i^{\text{Fe}}) + \frac{1}{2} \sum_{i \in \text{Cr}} \sum_{j \in \text{Cr}} \phi_{\text{Cr}}(r_{ij}), \\
 & + \sum_{i \in \text{Fe}} \sum_{j \in \text{Cr}} h\left(\frac{x_i + x_j}{2}\right) V_{\text{mix}}(r_{ij}),
 \end{aligned} \tag{42}$$

where we used the same notation as in the earlier sections. The partial electron densities  $\bar{\rho}_i^{\text{S}}$  follow the same definition as in Eq. (3). Furthermore, the local concentration variable  $x_i$  in Eq. (42) is defined as

$$x_i = \frac{\bar{\rho}_i^{\text{Cr}}}{\rho_i^{\text{Cr}} + \rho_i^{\text{Fe}}}. \tag{43}$$

The two densities  $\rho^{\text{Fe}}(r_{ij})$  and  $\rho^{\text{Cr}}(r_{ij})$  are normalised such that at the equilibrium lattice constant of each pure lattice, the respective partial electron density is 1. In this way the two EAM models for the pure elements are made compatible with each other.

Equation (42) looks quite similar to the composition-dependent pair potential energy expressions discussed in Sect. 2.1. There are, however, three essential differences: (i) There is only one mixed pair potential  $V_{\text{mixed}}(r_{ij})$  as opposed to two in Sect. 2.1 (one for each limit). (ii) There is no boundary conditions on the interpolation function  $h(x)$  at  $x = 0$  and  $x = 1$ . (iii) The local concentration about the  $(i, j)$  pair is just the average of the one-centre concentrations about the two sites, and not the two-centre concentration as defined in Eq. (9). Of course, at no extra cost the more rigorous definition in Eq. (9) is a better choice for the measure of local concentration about a pair of atoms. On the other hand, Eq. (8) shows that the one-centre concentration above is only a perturbation away from the more accurate quantity.

The Fe–Cr CD-EAM model was the pioneering work that has inspired the current paper. Here, we have tried to give a more rigorous foundation to the CD-EAM

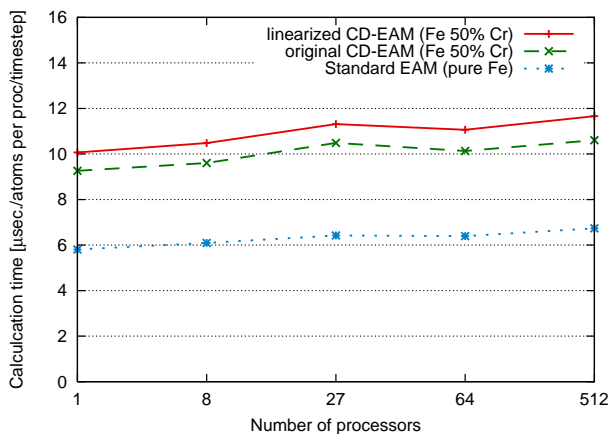


Figure 6. Comparison of the computation times for the CD-EAM models and the standard EAM model in a parallel molecular dynamics simulation. The benchmark simulation consists of a body-centred cubic crystal at 300 K with 16,000 atoms per processor.

model. In fact, we can strictly argue that CD-EAM is a simplified version of the current formalism. It works very well for the Fe–Cr system since the two elements are similar in size and chemical nature. It is therefore reasonable to make the approximation that functional forms of the mixed pair potentials describing the two dilute limits are the same.

Let us illustrate the last statement with the example of Lennard-Jones (LJ) potentials. These potentials are determined by two parameters:  $\sigma$  and  $\epsilon$ ; the first parameter specifies the position of the minimum of the potential or in other words the particle size, and the second parameter specifies the interaction strength. A mixture of two types of LJ particles with no size mismatch (same  $\sigma$ ) but different cohesive energies can be described by the same potential that is merely scaled differently for the two particles. Extending this analogy to the case of the Fe–Cr system we can see why only one mixed potential can be enough. However, it is important to realise now that when only one potential is used, the functions  $h(x)$  provide the interaction strength, which in the case of Fe–Cr is positive in one dilute limit and negative in the other. Hence no boundary conditions exist at the two concentrations  $x = 0$  and  $x = 1$ .

In the original CD-EAM model, there was a further simplification. The mixed potentials  $V_{\text{mix}}(r_{ij})$  was never fitted. In fact it was taken as the average of the effective EAM pairwise interactions of the pure elements at their respective equilibrium volumes

$$V_{\text{mix}}(r_{ij}) = \frac{1}{2} (\phi_{\text{Fe}}(r_{ij}) + 2U_{\text{Fe}}(\bar{\rho}_0^{\text{Fe}})\rho^{\text{Fe}}(r_{ij}) + \phi_{\text{Cr}}(r_{ij}) + 2U_{\text{Cr}}(\bar{\rho}_0^{\text{Cr}})\rho^{\text{Cr}}(r_{ij})), \quad (44)$$

where  $\bar{\rho}_0^{\mathcal{S}}$  is the electron density at the equilibrium lattice constant for the species  $\mathcal{S}$ . Only the function  $h(x)$  was fitted to the heat of mixing of the solid solution. The success of this model in spite of all the simplifications is a telltale of the power of this methodology.

## 6.2. Molecular dynamics and Monte Carlo performance

In Sect. 4 we presented an algorithm for calculating forces within the composition-dependent interatomic potential models which brings their efficiency on par with the standard EAM scheme. This was first discussed in a recent publication by the present authors [23], where this algorithm was implemented for the Fe–Cr CD-EAM



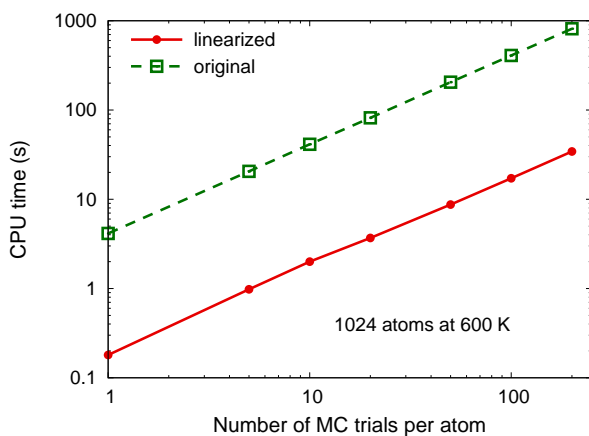


Figure 7. Comparison of the timing in a MC simulation of a Fe–Cr alloy at 50% composition. The simulation cell contained 1024 atoms.

model in the popular massively-parallel MD code LAMMPS [29]. To benchmark its performance, we carried out MD simulations of a body-centred cubic (BCC) crystal at 300 K using periodic boundary conditions. For the CD-EAM case we considered a random alloy with 50% Cr. For the standard EAM case, the sample contained only Fe. Simulations were run on 1, 8, 27, 64, and 512 processors with 16,000 atoms per processor (weak scaling). The results for the CD-EAM routines and the LAMMPS standard EAM routine are displayed in Fig. 6. In this figure, the original CD-EAM model as well as its linearised version are displayed. We see that the two versions are between 60% (linearised model) to 70% (original model) slower than the standard EAM. This is a small price to pay considering the fact that the CD-EAM expression actually contains explicit three-body forces.

In our recent publication [23] we also studied the Monte Carlo performance of composition-dependent interatomic potentials focusing on the comparison of the original and the linearised CD-EAM model. The performance gain due to the linearised formulation is illustrated in Fig. 7 which compares the timing of the linearised and original CD-EAM models in a serial MC simulation for a random Fe–Cr alloy at 50% composition. We find that the linearized CD-EAM model is twelve times faster than the original formulation. This is an impressive performance gain, which clearly advocates for linearised composition-dependent interatomic potentials.

## 7. Conclusions

The present work has come about in response to a need for a practical scheme for fitting interatomic potential models for multicomponent alloys. At this point of time, when faced with the task of modelling the chemistry of e.g. a ternary alloy, one is overwhelmed with the complexity of the problem. In this paper, we have presented a systematic methodology for the construction of alloy potentials, starting from pre-existing potentials for the constituent elements. The formalism represents a generalisation of the approach employed by one of the authors for the Fe–Cr system [13]. We have shown that this formalism naturally extends to treating multicomponent systems. The main idea of the approach is to describe the energetics of dilute concentrations of solute atoms in the pure host in terms of pair and higher-order cluster interactions (see Figs. 3 and 8). These interaction functions are then used as a basis set for expanding the potential energy of the alloy in the entire concentration range. To describe the energetics of the concentrated

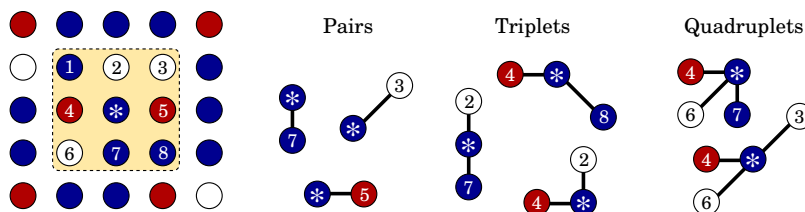


Figure 8. Several examples for clusters used to construct higher-order interaction terms which can be extracted from the configuration shown on the left.

alloys, the contributions of the basis functions are weighted by interpolation functions expressed in terms of local concentration variables. One of the innovations in this work is a novel measure of local composition around individual atoms in the system. This introduces an explicit dependence on the *chemical* environment. In this sense the composition-dependent interatomic potential scheme is reminiscent of the bond-order potential scheme developed by Abell and Tersoff [15–17] which employs a measure of the bond-order to distinguish between different *structural* motifs.

The main advantage of the framework presented here is that the basis functions can be constructed sequentially and independent of the interpolation functions, leading to a scheme that can be practically implemented and systematically improved upon. The lower order terms can be constructed with no knowledge of the higher order terms and therefore need not be reparametrised when higher order cluster potentials are constructed. The higher order terms in the expansion become progressively smaller. In this way the model can be made step by step, starting from the lowest order cluster potentials. Furthermore addition of new terms in the series expansion is not likely to introduce unphysical behaviour, a problem that plagues most fitting schemes for interatomic potentials.

The practical determination of the basis functions and the interpolation functions proceeds by fitting to first-principles data. The expansion in cluster interactions may be reminiscent of the celebrated “cluster expansion” technique [30] that has been used extensively during the past few decades to model the thermodynamics of multicomponent alloys from first principles. But it is important to note here that the methodology presented in this paper has no relation to the cluster expansion technique. The latter reduces the continuous phase space of e.g., a binary alloy onto the discrete configuration space of the corresponding Ising model. There is only one number associated with each cluster configuration, namely the the free energy of that cluster. The so-called “effective cluster interactions” (ECIs) are usually obtained via an optimisation process from all the cluster free energies. A procedure of the sort proposed in this paper is not possible, since there is not direct link between any single cluster free energy and an ECI. In contrast, when fitting e.g. a  $V_{AB}(r_{ij})$  interaction potential, a solute inclusion not only changes the total energy of the system, it causes forces in the system and modifies the force constants of the host, all of which can be used to construct a continuous pair potential.

Composition-dependent interatomic potentials are constructed by incorporating pair, triplet and higher-order cluster interactions that describe the energetics of clusters embedded in a pure host with a specific underlying lattice. One may now wonder, with this approach, could a potential be expected to handle systems which change lattice type as a function of concentration? For instance the Ni-Al phase diagram contains phases with BCC-based crystal structures, while the pure metals are face-centred cubic (FCC). Following the approach described above, the basis functions are parametrised in terms of solute cluster energies in the constituent FCC structures. How can one then expect to provide a reasonable model for the

BCC-based NiAl phase? The answer lies in the interpolation functions. They are fitted to the energetics of the ordered and disordered compounds along the concentration range with arbitrary crystal structures.

### Acknowledgements

Lawrence Livermore National Laboratory is operated by Lawrence Livermore National Security, LLC, for the U.S. DOE-NNSA under Contract DE-AC52-07NA27344. Partial financial support from the LDRD office and the Fusion Materials Program as well as computer time allocations from NERSC at Lawrence Berkeley National Laboratory are gratefully acknowledged.

### References

- [1] M. W. Finnis and J. E. Sinclair. A simple empirical  $N$ -body potential for transition metals. *Phil. Mag. A*, 50:45, 1984.
- [2] M. S. Daw and M. I. Baskes. Embedded-atom method: Derivation and application to impurities, surfaces and other defects in metals. *Phys. Rev. B*, 29:6443, 1984.
- [3] F Ercolessi, M Parrinello, and E Tosatti. Au(100) reconstruction in the glue model. *Surf. Sci.*, 177:314, 1986.
- [4] M. J. Puska, R. M. Nieminen, and M. Manninen. Atoms embedded in an electron gas: Immersion energies. *Phys. Rev. B*, 24:3037, 1981.
- [5] J. K. Norskov. Covalent effects in the effective-medium theory of chemical binding: Hydrogen heats of solution in the 3d metals. *Phys. Rev. B*, 26:2875, 1982.
- [6] S. M. Foiles, M. I. Baskes, and M. S. Daw. Embedded-atom-method functions for the fcc metals Cu, Ag, Au, Ni, Pd, Pt, and their alloys. *Phys. Rev. B*, 33:7983, 1986.
- [7] M. Ludwig, D. Farkas, D. Pedraza, and S. Schmauder. Embedded atom potential for Fe-Cu interactions and simulations of precipitate-matrix interfaces. *Modelling Simul. Mater. Sci. Eng.*, 6:19, 1998.
- [8] R. C. Pasianot and L. Malerba. Interatomic potentials consistent with thermodynamics: The Fe-Cu system. *J. Nucl. Mater.*, 360:118, 2007.
- [9] M. Asta and S. M. Foiles. Embedded-atom-method effective-pair-interaction study of the structural and thermodynamic properties of Cu-Ni, Cu-Ag, and Au-Ni solid solutions. *Phys. Rev. B*, 53:2389, 1996.
- [10] E. Ogando Arregui M. Caro and A. Caro. Numerical evaluation of the exact phase diagram of an empirical Hamiltonian: Embedded atom model for the Au-Ni system. *Phys. Rev. B*, 66:054201, 2002.
- [11] Y. Mishin, M. J. Mehl, and D. A. Papaconstantopoulos. Embedded-atom potential for B2-NiAl. *Phys. Rev. B*, 65:224114, 2002.
- [12] Y. Mishin. Atomistic modeling of the  $\gamma$  and  $\gamma'$ -phases of the NiAl system. *Acta Mater.*, 52:1451, 2004.
- [13] A. Caro, D. A. Crowson, and M. Caro. Classical many-body potential for concentrated alloys and the inversion of order in iron-chromium alloys. *Phys. Rev. Lett.*, 95:075702, 2005.
- [14] P. Olsson, J. Wallenius, C. Domain, K. Nordlund, and L. Malerba. Two-band modeling of  $\alpha$ -prime phase formation in Fe-Cr. *Phys. Rev. B*, 72:214119, 2005.
- [15] G. C. Abell. Empirical chemical pseudopotential theory of molecular and metallic bonding. *Phys. Rev. B*, 31:6184, 1985.
- [16] J. Tersoff. New Empirical Model for the Structural Properties of Silicon. *Phys. Rev. Lett.*, 56:632, 1986.
- [17] J. Tersoff. New empirical approach for the structure and energy of covalent systems. *Phys. Rev. B*, 37:6991, 1988.
- [18] M. Müller, P. Erhart, and K. Albe. Thermodynamics of L1<sub>0</sub> ordering in FePt nanoparticles studied by Monte Carlo simulations based on an analytic bond-order potential. *Phys. Rev. B*, 76:155412, 2007.
- [19] M. I. Baskes. Application of the embedded-atom method to covalent materials: A semiempirical potential for silicon. *Phys. Rev. Lett.*, 59:2666, 1987.
- [20] M. I. Baskes. Modified embedded-atom potentials for cubic materials and impurities. *Phys. Rev. B*, 46:2727, 1992.
- [21] F. H. Stillinger and T. A. Weber. Computer simulation of local order in condensed phases of silicon. *Phys. Rev. B*, 31:5262, 1985.
- [22] M. S. Daw, S. M. Foiles, and M. I. Baskes. The embedded-atom method - A review of theory and applications. *Mater. Sci. Rep.*, 9:251, 1993.
- [23] A. Stukowski, B. Sadigh, P. Erhart, and A. Caro. Efficient implementation of the concentration-dependent embedded atom method for molecular dynamics and Monte-Carlo simulations. *Modelling Simul. Mater. Sci. Eng.*, 17:075005, 2009.
- [24] A. Caro, M. Caro, E. M. Lopasso, and D. A. Crowson. Implications of ab initio energetics on the thermodynamics of Fe-Cr alloys. *Appl. Phys. Lett.*, 89:121902, 2006.

- [25] P. Erhart, A. Caro, M. Serrano de Caro, and B. Sadigh. Short-range order and precipitation in Fe-rich Fe–Cr alloys. *Phys. Rev. B*, 77:134206, 2008.
- [26] P. Olsson, I. A. Abrikosov, L. Vitos, and J. Wallenius. Ab initio formation energies of Fe–Cr alloys. *J. Nucl. Mater.*, 321:84, 2003.
- [27] P. Erhart, B. Sadigh, and A. Caro. Are there stable long-range ordered  $\text{Fe}_{1-x}\text{Cr}_x$  compounds? *Appl. Phys. Lett.*, 92:141904, 2008.
- [28] T. P. C. Klaver, R. Drautz, and M. W. Finnis. Magnetism and thermodynamics of defect-free Fe–Cr alloys. *Phys. Rev. B*, 74:094435, 2006.
- [29] S. Plimpton. Fast parallel algorithms for short-range molecular dynamics. *J. Comp. Phys.*, 117:1, 1995.
- [30] J. M. Sanchez, F. Ducastelle, and D. Gratias. Generalized cluster description of multicomponent systems. *Physica A*, 128:334, 1984.